

Investigation of Static Voltage Accumulation on Wind Turbine Blade in Atmospheric Wind speed Humidity and Temperature

Abstract. Wind turbines are one of renewable energy sources. Wind turbines installed at wild open area such offshore, mountains and deserts are filled with air particles and flow of wind speed. During the wind flow throughout the wind turbines which rotates the turbine blades, there is friction between the air particles and the blade surface that leads the static voltage to accumulate on the blade surface causing upward streamers. Using fiberglass reinforced plastic (FRP) wind turbine blades by simulation and experimental method. The charged particle tracing with electrostatics and laminar flow with time-dependent used to determine the value of static voltage accumulation. Static voltage accumulation is influenced by various factors such as wind speed (1, 5, and 7 m/s), humidity (20, 50, and 70 %RH) and temperature (28, 35, and 48 oC) had tested and analyzed. Furthermore, the result obtained using the Finite Element Method (FEM) has shown a good agreement with the experimental result. It was observed that high flow velocity has a great tendency to charge the blade surface with 36.70% higher from 1 m/s to 7 m/s. Low relative air humidity increases the risk of static electricity 221.6 V at the of side of the blade when humidity is 20%. Moreover, increasing the air temperature from 28 to 48 degrees Celsius increases the voltage by 20%. Therefore, determining the need for static voltages generated in the blade surface and the risk related to upward streamers is obliged to be evaluated as it is the essential ways in adopting the correct protection systems.

Streszczenie. Turbiny wiatrowe są jednym z odnawialnych źródeł energii. Turbiny wiatrowe zainstalowane na dzikich terenach otwartych, takich jak wybrzeże, góry i pustynie, są wypełnione cząsteczkami powietrza i prędkością wiatru. Podczas przepływu wiatru przez turbiny wiatrowe, który obraca łopaty turbiny, występuje tarcie między cząstkami powietrza a powierzchnią łopaty, co prowadzi do gromadzenia się napięcia statycznego na powierzchni łopaty, powodując wznoszenie się wstęg. Wykorzystanie łopat turbin wiatrowych z tworzywa sztucznego wzmocnionego włóknem szklanym (FRP) za pomocą modelowania i metody eksperymentalnej. Śledzenie cząstek naładowanych za pomocą elektrostatyki i przepływu laminarnego z zależnym od czasu wykorzystaniem do wyznaczania wartości kumulacji napięcia statycznego. Na akumulację napięcia statycznego mają wpływ różne czynniki, takie jak prędkość wiatru (1, 5 i 7 m/s), wilgotność (20, 50 i 70 %RH) oraz temperatura (28, 35 i 48 oC). Ponadto wynik uzyskany metodą elementów skończonych (MES) wykazał dobrą zgodność z wynikiem doświadczalnym. Zaobserwowano, że duża prędkość przepływu ma dużą tendencję do obciążania powierzchni łopaty o 36,70% większą od 1 m/s do 7 m/s. Niska wilgotność względna powietrza zwiększa ryzyko powstania elektryczności statycznej 221,6 V z boku łopaty, gdy wilgotność wynosi 20%. Ponadto zwiększenie temperatury powietrza z 28 do 48 stopni Celsjusza powoduje wzrost napięcia o 20%. W związku z tym określenie konieczności występowania napięć statycznych generowanych na powierzchni łopaty oraz zagrożenia związanego ze skierowanymi w górę streamerami wymaga oceny, ponieważ jest to niezbędny sposób w doborze odpowiednich systemów ochronnych. (Badanie akumulacji napięcia statycznego na łopatach turbiny wiatrowej przy prędkości wiatru atmosferycznego, wilgotności i temperaturze)

Keywords: CFD, Static Voltage Accumulation, Electrical field, lightning Protection.

Słowa kluczowe: CFD, akumulacja napięcia statycznego, pole elektryczne, ochrona odgromowa.

Introduction

Renewable energy has been developing rapidly over recent years because it is clean and environment friend generation method. According to According to Global Wind Energy Council (GWEC) figures, the global yearly installed wind capacity in 2016 is 54.642 GW and 90 GW on 2020, while the global total installed wind capacity through 2016 is 486.790 GW and 707GW on 2020 [1], [2].

Everything around us has affected by triboelectric or static electricity. One of the simplest examples is walking on a carpet and then feeling shocked when the hand touches the doorknob. This is how the surfaces get contact electrification from rubbing with other surfaces [3]–[5].

Wind turbines are tall structures exposed to wind flow constantly. Wind turbine installation areas such as offshore, mountains, and deserts are filled with air particles and flow with wind speed [6], [7]. During this process, which rotates the turbine blades, there is friction between the air particles and the blade surface that leads the charge to accumulate on the blade surface causing upward streamers. Solid particles in a gaseous flow system are naturally charged due to the friction and collisions between the surface of different particle materials [8]–[14].

Electrostatics voltage are the generation of static electricity when two objects with a different or same material rub against each other. The separation of positive and negative charges is one of the requirements for the static electricity phenomena.

Moreover, other natural processes, such as liquid or solid separation, air, and particle ionization, can also

generate electrostatic charges. When the air flows in the atmosphere, free electrons had generated continuously. As they are generated, they remain free for a short time on the order of tens of nanoseconds because they become attached to oxygen molecules in the air. Because of their small mass, the electrons accelerate rapidly, gaining energy [13]. Through years of study, the general idea of the phenomenon of static electricity related to particles and air is not well understood [14]. However, no research or studies discussed the static voltage accumulation on wind turbine blades.

The electrostatic charge that occurs by airflow depends on the nature of the surface, flow conditions, and the number of particles flying through the surface. Computational Fluid Dynamics (CFD) is considered necessary in fluid flow simulation and has recently gained interest in solving complex operations in the field of air particle flow and its properties. Here we have investigated static voltage accumulation on wind turbine blades under several factors, airspeed, humidity, and temperature. simulation using the Finite Element Method (FEM) and experiments have been performed with different combinations of operating conditions.

Simulation

The computational domain size of 1 m × 2 m was selected to model the electrostatic voltage accumulation on the wind turbine blade. A 1.7 m Fiber Glass Epoxy wind turbine blade has been used in this simulation. Fig. 1 shows

the computational domain divided into two parts; the first part is the ionization process between air particles, and the second part is the charges particle flow throughout the blade.

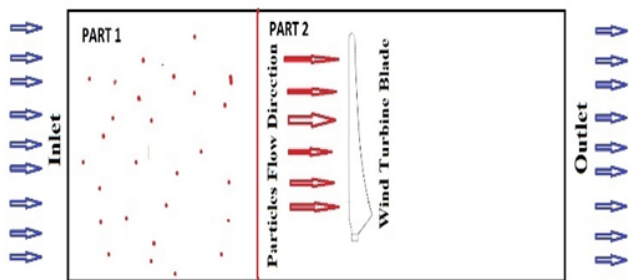


Fig. 1. Two components of the computational domain; part 1 ionization process and part 2 charge interaction with the blade

Navier-Stokes's equation-based laminar airflow is applied at the inlet part with three different velocities 1, 5, and 7 (m/s) [15]. Navier-Stokes's equation is a partial differential equation that describes the motion of particles and mathematically expresses the conservation of momentum and mass for Newtonian fluids.

$$(1) \quad \rho \frac{Du}{Dt} = \rho \left(\frac{\partial u}{\partial t} + (\mathbf{u} \cdot \nabla) \mathbf{u} \right) = -\nabla P + \nabla \cdot \left[\mu \left(\nabla \mathbf{u} + (\nabla \mathbf{u})^T - \frac{2}{3} (\nabla \cdot \mathbf{u}) \mathbf{I} \right) \right] + F$$

Where \mathbf{u} is the fluid velocity vector, P is the fluid pressure, ρ is the fluid density in kg/m^3 , μ is the dynamic fluid viscosity, and F is the external force. Table 1 shows the parameters used in computational fluid dynamics with charged particle tracking. The Navier-Stokes equations indicate momentum conservation, whereas the continuity equation represents mass conservation. Therefore, Navier-Stokes and the continuity equations are always solved together.

$$(2) \quad \frac{\partial \rho}{\partial t} + \nabla \cdot (\rho \mathbf{u}) = 0$$

The Navier-Stokes equations represent the conservation of momentum, while the continuity equation represents the conservation of mass. These equations are essential in fluid flow simulation, and we use them to solve a particular set of boundary conditions such as inlets, outlets, and walls. The Reynolds numbers in $Re = \rho U L / \mu$ are the ratio of internal forces in $\rho \left(\frac{\partial \mathbf{u}}{\partial t} + (\mathbf{u} \cdot \nabla) \mathbf{u} \right)$ to the viscous forces in Eq. (3). Low Reynolds number flows are laminar flows, while Higher Reynolds number flows are turbulent.

$$(3) \quad \nabla \cdot \left[\mu \left(\nabla \mathbf{u} + (\nabla \mathbf{u})^T - \frac{2}{3} (\nabla \cdot \mathbf{u}) \mathbf{I} \right) \right]$$

Table 1 simulation parameters

Name	Value	Description
U	1, 5, 7 (m/s)	Inlet velocity
T₀	28, 35, 48 (°C)	Temperature
RH	20%, 50%, 70%	Humidity
Mw	0.028 kg/mol	Molecular weight
p_{in}	0.001 Pa	inlet pressure
M	4.6495E-2 kg	Particle mass
J_{in}	2.9082E19 1/(m ² ·s)	Emitted molecular flux
Np	10000	Number of particles

Part 1: Gas ionization

The physics interface formulation used in this simulation is Newtonian, used to simulate the motion of particles in the fluid. A particle-particle interaction node has used to make particles exert forces on each other. A system N of charges q_i at the direction r_i the generated electric field, which magnitude and direction are by superposition as in Eq. (4):

$$(4) \quad E(r) = \frac{1}{4\pi\epsilon_0} \sum_{i=1}^N q_i \frac{r-r_i}{|r-r_i|^3}$$

Part 2: Particle interaction with blade

Part 2 of the computational domain include the wind turbine blade and the motion of particle flowing throughout the blade structure. Eq. (4) represents Coulomb's law to describe the interaction between charged particles. The simulation used is for continuum and free molecular flow. The ionic charging of particles is usually known as diffusion or field charging. Diffusion charging occurs when the particle acquires a charge based on the random thermal motion of ions and their collision and adherence to the particles. A friction force nod has been added to this part, defining it as the domain dimension's step function. This function describes the friction between particles and the wall structure (wind turbine blade) and the speed of particles. Eq. (5):

$$(5) \quad F = -m_p \nu (\mathbf{v} - \mathbf{u})$$

A particle mass $-m_p$; with collision frequency ν at the opposite direction of friction force, \mathbf{v} is particles velocity, and \mathbf{u} is fluid flow velocity. After compiling all these physics together, it will be possible to measure the voltage accumulated by charges of particles and the friction with the blade surface through the cutline is shown in Fig 2.

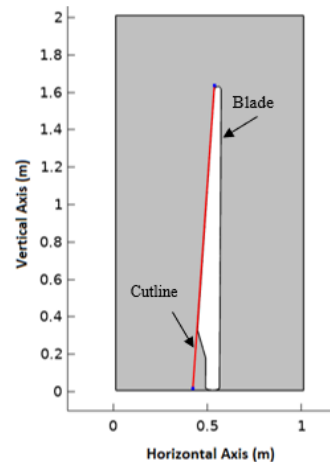


Fig. 2. Cut-line define for measuring electrostatic voltage

Experimental setup

We built the chamber to set up the appropriate environment for measuring the static electricity accumulated from the wind turbine blade.

Blade

The wind turbine blade's design compromises structural and aerodynamic factors. The design of the outer two-thirds of the blade is often dominated by aerodynamic characteristics, whereas structural elements typically dominate the interior one-third of the blade. Therefore, materials used to build wind turbine blades require low density, high strength, fatigue resistance, and damage tolerance [16], [17].

A 1.7 m length with three layers of fiberglass material was used to build the wind turbine blade tip [1], as shown in Fig 3. The blades made from fiberglass risen epoxy are

considered a non-conductive material. Therefore, it needs a long time to gain static electricity, and it is not easy to discharge them; see electrical parameters of fiberglass resin epoxy used in this study Table 2:

Table 2 Electrical parameters of Fiberglass resin epoxy

Property	Description	Value
σ	Conductivity	0.004 S/m
Y	Young's module	30.90 GPa
ν	Poisson ratio	0.0866
ρ	Density	1800 kg/m ³

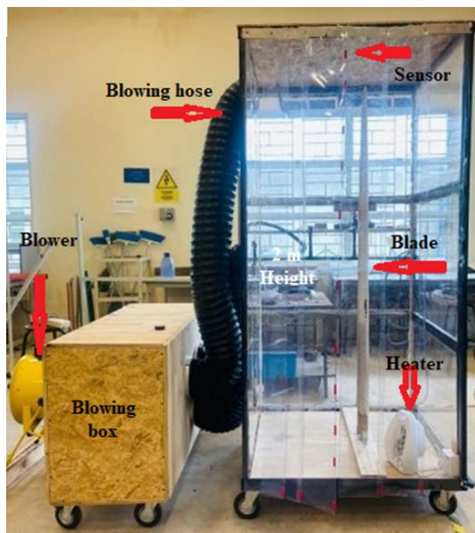


Fig. 3. Wind turbine blade used in the experiment

In this experiment, three different areas were used to collect the measurement, Top, Middle, and Bottom, as in Fig. 3.

Chamber

This work uses the chamber to evaluate the impact of specific environmental conditions like temperature, humidity, and airflow. The dimensions of a chamber designed to fit with the blade length. The height of the chamber is 2 m, while the length and width are 1m, respectively shown in Fig 4.



(a)

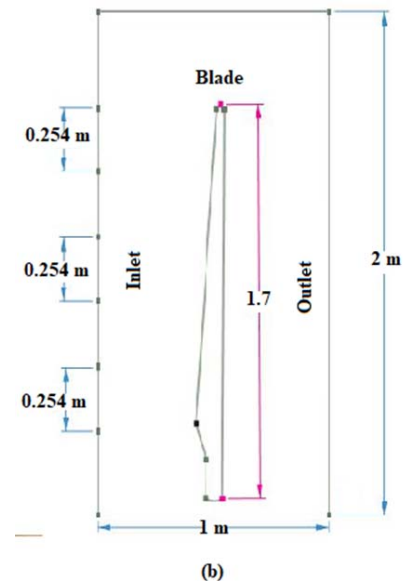


Fig. 4. The experiment chamber (a) physical view (b) Dimension

Experiment Process

Fig. 5. represents the experiment process, the devices used in this experiment to generate airflow with the required factors are controlled by the control panel. For the airflow, we used a 12-inch ventilation fan with 2900 r/m blowing inside the blowing box in Fig. 4. The blowing box is connected to the chamber using three 10-inch (25.6 cm) holes connected to the chamber by a hose. Through this stage, air flows to the top, middle, and bottom of the blade, and the fan speed is controlled using a voltage regulator controller and the air speed measured by Anemometer with a measurement range from 0.4 m/s to 30 m/s.

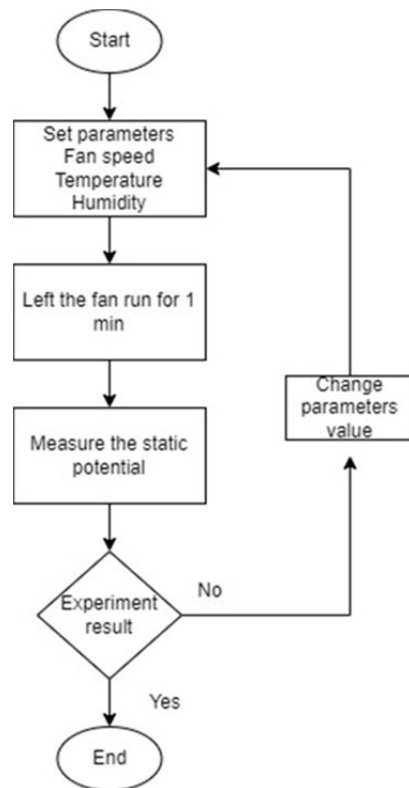


Fig. 5. Experiment Process Flow

A temperature and humidity sensor controller PID will detect and control the temperature and humidity inside the

chamber according to the setting value. Electrostatic Sensor KEYENCY SK-H050 measured the static voltage accumulation.

Result and Discussion

Flow velocity

The particle flow and electrical properties has used to investigate the accumulated static voltage on the wind turbine blade. The wind flow speed, humidity, and temperature involved in the chamber to analyse and measure the amount of static voltage accumulated on the wind turbine blade.

Fig. 6 shows the velocity magnitude throughout the blade. The velocity increases at the tip part of the blade. At the same time, the flow of wind carrying air particles has concentrated in the upper part of the blade, this area sensitive to the friction of these particles with the blade surface.

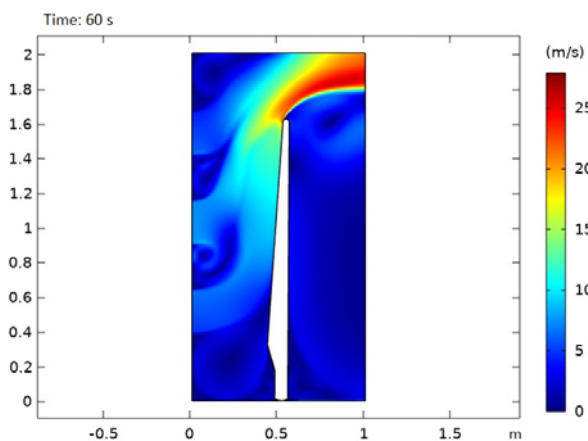


Fig. 6. The velocity of airflow onto the blade in simulation

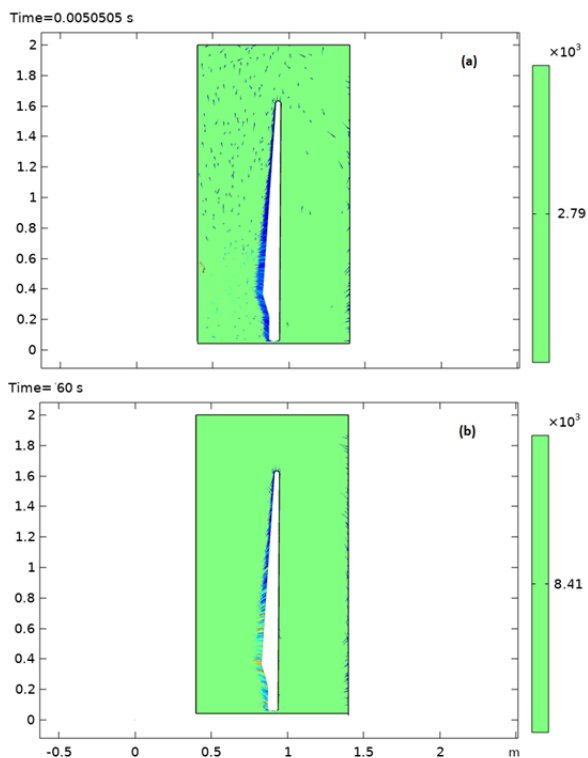


Fig. 7. Particle accumulation number with time at (a) 0.005 s and (b) 60 s in simulation

Wind velocity, number of accumulated particles, humidity, and temperature are the main factors that static

electricity depends on it. Fig 7 shows the particles collected on the blade surface with time. Fig. 7 (a) shows the particle flow at 0.005s; in the first step of particle flow time, 2.79×10^3 particles accumulated on the blade surface compared with the flow at 60 seconds, which has 8.41×10^3 particles in Fig. 7 (b).

The accumulated static voltage increases when airflow velocity and number of charged particles increases. Meanwhile, at high humidity the accumulated static voltages becomes lower [7], [18].

Table 3 Measured electrostatic voltage for three airflow velocities

AREA	Velocity					
	1 m/s		5 m/s		7 m/s	
	Exp.	Simu.	Exp.	Simu.	Exp.	Simu.
Top	97.1	83.3	113	104.2	132	145.9
Middle	67.2	53.06	97.6	66.3	102.8	92.8
Bottom	36.6	51.9	64.8	64.9	81.4	90.8

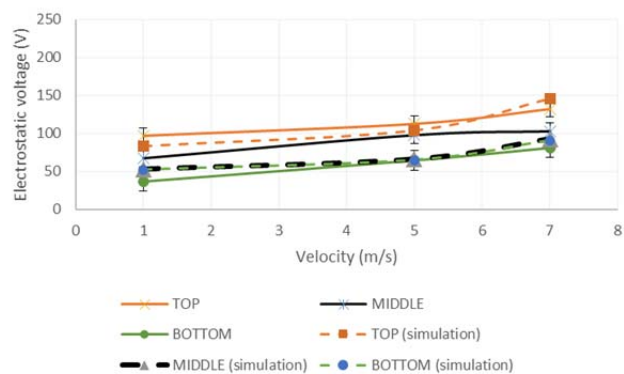


Fig. 8. Electrostatic voltage accumulation with flow velocity simulation and experimental result

Fig. 8 shows the behavior of electrostatic voltage with respect to changes in wind flow velocity. The solid line is the experimental value, and the dotted lines are the calculated value. The figure shows that the static voltage increases with the increase in wind flow velocity. Also, the measured static voltages are in good agreement with the calculated values. This indicates that the number of accumulated charges increases with wind flow speed.

The first indication of wind-speed-dependent charging phenomena such as lightning. It was observed from Fig. 8 the airflow speed affects the static voltage accumulation on a wind turbine blade. The electrostatic voltage measured along the side of the wind flow with the cutline, as shown in Fig. 2, showed that the electrostatic voltage increases at the top of the blade, coinciding with the rise of wind velocity and particle flow in this region. In contrast, the wind speed increase at the blade's top part gives the highest measure of static voltage compared with the middle and bottom sides, as shown in Table 3.

Humidity

Fig. 9 describes the humidity behavior on the blade's electrostatic voltage accumulation on the surface of a $28\text{ }^{\circ}\text{C}$ temperature environment. Each circular data is an average of five tested experiment samples with the error bars showing deviating values.

The results from the experiment values, and the simulation values which offer a good agreement between experiment and simulation results. There is an inverse relationship between the percentage of humidity and the electrostatic voltage generated by the blade surface. In comparison, 20% of humidity gives the highest voltage at the top of the blade compared with the middle and bottom region, which provides lower voltage charges.

The 70% humidity indicator gave the lowest percentage of electrostatic voltage measurements on the blade surface compared with 50% and 20%, respectively.

Table 4. Electrostatic and calculated voltage for different humidity

Area	Humidity					
	20%		50%		70%	
	Exp.	Mod.	Exp.	Mod.	Exp.	Mod.
Top	221.6	216.05	121.8	122	59.8	75.3
Middle	171	141.07	68.2	89.5	39.6	51.3
Bottom	92.2	129.8	57.4	80.5	31.2	46.7

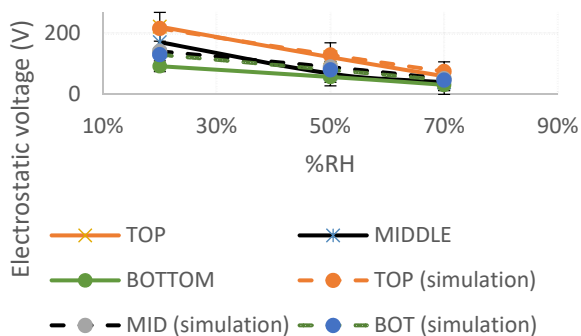


Fig. 9. Electrostatic voltage accumulation with humidity simulation and experimental result.

Temperature

As discussed above, electrostatic accumulates on surfaces with highly insulating materials and slowly gaining charge depends on the surrounding atmosphere. Fig. 10 that the blade surface has high static voltages generation at a high degree Celsius.

The influence of temperature on static voltage accumulation on the blade surface is clear. Fig. 12 represents the experiment and simulation results, which clearly shows that the static voltage accumulation at 48 C° gives the highest record of charging voltage at the three-blade portions.

The comparison can be made from Table 5; the difference between experimental and simulation results is estimated to be 3.23% to 20%. Therefore, the higher the temperature, the higher chance of charging the surface, and temperature changes can generate a temporary voltage [4].

Table 5 Electrostatic and calculated voltage for different temperature

Area	Temperature					
	28 C°		35 C°		48 C°	
	Exp.	Mod.	Exp.	Mod.	Exp.	Mod.
Top	104	95.8	165	145	204	198
Middle	76.4	61.2	89.8	92.8	161	128
Bottom	62.6	59.7	68.2	72.7	81	91.8

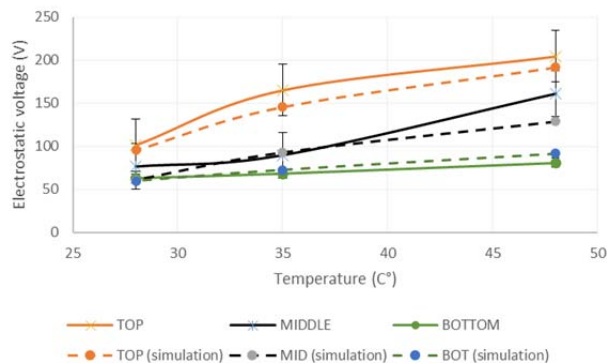


Fig. 10. Electrostatic voltage accumulation with temperature simulation and experimental result.

Conclusion

Wind turbines generate electricity when the wind pass through the blades causing the rotation process. During this process, which rotates the turbine blades, there is friction between the air particles and the blade surface that leads the static voltage to accumulate on the blade surface causing upward streamers. Therefore, measuring the static voltage accumulate on wind turbine blade under various environment condition could be easy to know the phenomenon of upward streamers.

The electrostatic charging on fiberglass epoxy material depends on the surrounding environmental factors. Therefore, we experiment and FEM simulation to characterize the static voltage accumulation of wind turbine blades with particles flowing under different wind speed levels, temperatures, and humidity.

The flow of wind speed throughout the wind turbine blade significantly affects static voltage accumulation. For example, increasing wind speed from 1 m/s to 7 m/s can charge the blade surface to 36.70 %.

The effect of humidity gave a high and close reading between simulation and experiment. The highest reading recorded is 221.6 V at the top of the blade when the humidity is low (20%) in the air compared with temperature. Low relative air humidity increases the risk of static electricity.

The simulation and experiment results in convergence show that increasing the air temperature from 28 to 48 degrees Celsius increases the voltage by 20%.

From the results obtained, it's clear to see that the top part of the blade has the highest electrostatic voltage compared with the middle and bottom pieces. The increase of electrostatic voltage is contributed to the air and particles' flow being high at the top of the blade [19].

Future work, how to remove this static voltage from blade surface to avoid lightning attachment to the blade.

Acknowledgment

The authors would like to thank University Malaysia Pahang for providing financial support under Research Grant (University reference RDU210320 and PDU223206), and financial support under Collaborative Research Grant with University Technology Malaysia (RDU192324, No. J130000.7351.4B483).

REFERENCES

- [1] Q. Zhou, C. Liu, X. Bian, K. L. Lo, and D. Li, "Numerical analysis of lightning attachment to wind turbine blade," *Renew. Energy*, vol. 116, pp. 584–593, 2018, doi: 10.1016/j.renene.2017.09.086.
- [2] W. Yu, Q. Li, J. Zhao, H. Li, and W. H. Siew, "Thundercloud-induced spatial ion flow in the neighborhood of rotating wind turbine and impact mechanism on corona inception," *IEEE Trans. Plasma Sci.*, vol. 49, no. 9, pp. 2925–2935, 2021, doi:

- 10.1109/TPS.2021.3102376.
- [3] D. J. Lacks and R. Mohan Sankaran, "Contact electrification of insulating materials," *J. Phys. D: Appl. Phys.*, vol. 44, no. 45, 2011, doi: 10.1088/0022-3727/44/45/453001.
- [4] D. P. Nolan, "Control of Ignition Sources," *Handb. Fire Explos. Prot. Eng. Princ. Oil, Gas, Chem. Relat. Facil.*, pp. 251–270, 2019, doi: 10.1016/b978-0-12-816002-2.00014-3.
- [5] C. Heinert, R. M. Sankaran, and D. J. Lacks, "Microscale Bipolar Charge Distributions on Surfaces after Liquid Wetting and Evaporation in an Electric Field," *Langmuir*, vol. 37, no. 26, pp. 8007–8013, 2021, doi: 10.1021/acs.langmuir.1c01052.
- [6] S. Matsusaka, H. Umamoto, M. Nishitani, and H. Masuda, "Electrostatic charge distribution of particles in gas-solids pipe flow," *J. Electrostat.*, vol. 55, no. 1, pp. 81–96, 2002, doi: 10.1016/S0304-3886(01)00185-1.
- [7] T. A. L. Burgo, C. A. Silva, L. B. S. Balestrin, and F. Galebeck, "Friction coefficient dependence on electrostatic tribocharging," *Sci. Rep.*, vol. 3, pp. 1–8, 2013, doi: 10.1038/srep02384.
- [8] Z. Guo *et al.*, "The influence of the metal mesh to the attachment manner of cfrp wind turbine blades," *2019 11th Asia-Pacific Int. Conf. Light. APL 2019*, no. October 2020, 2019, doi: 10.1109/APL.2019.8816011.
- [9] W. Rison *et al.*, "Observations of corona discharges from wind turbines," *IET Semin. Dig.*, vol. 2015, no. 11, 2015, doi: 10.1049/ic.2015.0195.
- [10] H. Photoionizers, "New choices for removing static charges . X-rays are what make it possible ! Photoionization mechanism".
- [11] E. S. P. B. V, S. Nieh, and T. Nguyen, "E f f e c t s of h u m i d i t y , c o n v e y i n g v e l o c i t y , a n d p a r t i c l e s i z e o n e l e c t r o s t a t i c c h a r g e s o f g l a s s b e a d s i n a g a s e o u s s u s p e n s i o n f l o w," vol. 21, pp. 99–114, 1988.
- [12] J. R. Toth *et al.*, "Electrostatic forces alter particle size distributions in atmospheric dust," *Atmos. Chem. Phys.*, vol. 20, no. 5, pp. 3181–3190, 2020, doi: 10.5194/acp-20-3181-2020.
- [13] V. Cooray, *An introduction to lightning*. 2015. doi: 10.1007/978-94-017-8938-7.
- [14] P. Zilio, W. Raja, A. Alabastri, F. De Angelis, and R. P. Zaccaria, "Modeling of space-charge effects in thermionic devices," vol. 1576, no. October 2015, pp. 3–4, 2016.
- [15] D. Horia, C. Vladimir, D. Alexandru, and F. Florin, "The laminar boundary layer on a rotating wind turbine blade," *Incas Bull.*, vol. 2, no. 2, pp. 40–49, 2010, doi: 10.13111/2066-8201.2010.2.2.6.
- [16] V. Christensen, "Ecopath with Ecosim: linking fisheries and ecology 1 Why ecosystem modeling in fisheries?," *WIT Trans. State Art Sci. Eng.*, vol. 34, pp. 1755–8336, 2009, doi: 10.2495/978-1-84564.
- [17] S. A. Pastromas, K. Sandros, K. N. Koutras, and E. C. Pyrgioti, "Investigation of lightning strike effects on wind turbine critical components," *ICHVE 2018 - 2018 IEEE Int. Conf. High Volt. Eng. Appl.*, no. November 2019, pp. 1–4, 2019, doi: 10.1109/ICHVE.2018.8642050.
- [18] Z. Qiao, Z. Wang, C. Zhang, S. Yuan, Y. Zhu, and J. Wang, "PVAm-PIP/PS composite membrane with high performance for CO₂/N₂ separation," *AIChE J.*, vol. 59, no. 4, pp. 215–228, 2012, doi: 10.1002/aic.
- [19] D. M. Taylor, "Measuring techniques for electrostatics," *J. Electrostat.*, vol. 51–52, no. 1–4, pp. 502–508, 2001, doi: 10.1016/S0304-3886(01)00107-3.